Surface Orientation Recovery of Specular Micro-surface via Binary Pattern Projection

[1]*Zhan Song,* [1]*Ronald Chung*[*], [1]*Jun Cheng,* [2]*Edmund Y. Lam*

[1]Dept. of ACAE, The Chinese University of Hong Kong, Hong Kong, China
[2]Dept. of EEE, The University of Hong Kong, Hong Kong, China

ABSTRACT

With the continuous effort of the electronic industry in miniaturizing device size, the task of inspecting the various electrical parts becomes increasingly difficult. For instance, solder bumps grown on wafers for direct die-to-die bonding need to have their 3D shape inspected for assuring electrical contact and preventing damage to the processing equipments or to the dies themselves in the bonding process. Yet, the inspection task is made difficult by the tiny size and the highly specular and textureless nature of the bump surfaces. In an earlier work we proposed a mechanism for reconstructing such highly specular micro-surfaces as wafer bumps. However, the mechanism is capable of recovering 3D positions only. In this paper we describe a new mechanism that recovers surface orientations as well which are as important in describing a surface. The mechanism is based upon projecting light from a point or parallel light source to the inspected surface through a specially designed binary grid. The grid consists of a number of black and transparent blocks, resembling a checker board. By shifting the grid in space a number of times in a direction not parallel to either boundary of the grid elements, and each time taking a separate image of the illuminated surface, we could determine the surface orientations of the inspected surface at points which appear in the image data as grid corners. Experimental results on real objects are shown to illustrate the effectiveness of the proposed mechanism.

Keyword: Surface Orientation, Specular Surface, Structured Light, Checker Board Pattern, Grid Corners.

1. INTRODUCTION

Recovery of surface orientation is an interesting topic in computer vision. Its importance in general comes from its various applications in different regions, including surface registration and matching [1], pose estimation [2], object recognition [3, 4] and so on. Surface normal, an important basis of robust 3D feature determination, is not only used to represent surface orientation but also can be used to reconstruct the surface itself. Such as shape from shading [5], shape from texture [6]. The determination of surface orientation from texture cues has been based on two general techniques. Gradient methods, exemplified by the work of Gibson, rely on changes in texture properties such as the density of texture as the surface recedes from the observer. It is also possible, to deduce surface orientation from purely local properties of the observed texture [7, 8]. However, the surface normals obtained from these methods are usually ill-conditioned and sensitive to noise.

Reconstruction of surface orientation has also been researched in the structured light projection. In the method proposed by Neelima Shrikhande and George Stockman [9], a grid pattern is projected onto an object. Surface normals at intersection points are induced from the deformation of the grid edge lengths. The result illustrates that it will cause big errors if the grid cell edges have big distortion like the sharp edges. Woodham [10] proposed a photometric stereo method which determines the surface orientation of each point by changing the source direction. Sugihara [11] proposed a method which infers local surface orientation using the distortion of a known pattern projected on the object surface from a structured light source. The projected textures on the object surface are detected and the distortion from the regular pattern is measured in order to estimate the surface orientation. S. Winkelbach and F. M. Wahl [12] used a uni-direction strip pattern to compute the surface normal at each edge point. The fringe pattern is projected onto the object twice with two different angles, two surface tangents are obtained. Surface normal at every image point can be interpolated by the

[*] Further author information: Ronald Chung (E-mail: rchung@acae.cuhk.edu.hk) is the correspondence author.

Machine Vision Applications in Industrial Inspection XIV, edited by Fabrice Meriaudeau, Kurt S. Niel,
Proc. of SPIE-IS&T Electronic Imaging, SPIE Vol. 6070, 60700S, © 2006 SPIE-IS&T · 0277-786X/06/$15

two angle images. A simplified method which determines the surface orientation of an object by estimating the surface normals from the slopes and intervals of the stripes in the image was also proposed [13, 14]. It is based on the assumption that the surface between two strip edges is planar or very smooth. So the tilt angle can be estimated from deformed strip widths by comparing them with the strip width measure in reference plane.

Solder inspection has been an application of particular interest since it is a common industrial task which is also very laborious due to the size and nature of surface. Not only the shape but also orientation recovery of the solder suffers from these features. Light projected onto the solder surface will make saturation regions, and the light projected onto the substrate is absorbed mostly. The confused intensity information on the surface makes it almost impossible to recover the shape or orientation from gray level. The structured light inspection of the specular surface has also been attempted. In the method proposed Arthur C. Sanderson, a scanned array of point sources and images of the resulting reflected highlights to compute local surface height and orientation [15]. But it still need big improvement and far away from application.

In this paper, we proposed to use a checker board pattern instead of a strip pattern as shown in Figure 1. In the pattern, two black or white blocks intersect at one point referred to as grid point. To each grid point, there are two sharp edges where the intensity changes from black to white and vice versa. When it is projected onto the object surface, these edges will be modulated by the surface shape. And the surface tangents can be calculated from the local edge directions. From single projection, we can get two surface tangents in different directions. Different from the orientation recovery methods based on local image intensity, our method depends on the structure - block boundary. Compared with the methods based on fringe pattern projection, two surface tangents are used at the same time. So, it is more accurate and reliable except the sparse data density. But in our approach, it can be resolved by shifting the pattern. Consider the saturation caused by specular surface, a robust local grid corner and surface tangent detection method has also been proposed. The experimental results show that most of the grid corners and tangents can be detected effectively.

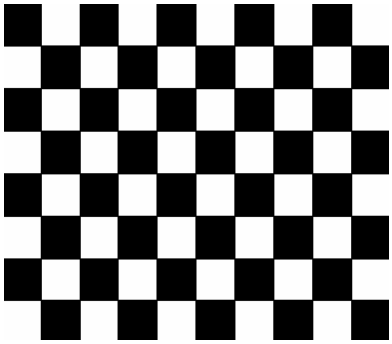

Figure 1. A checker board pattern.

In Section 2, the principle of surface normal from two tangents is introduced. The formula is derived, and the parameters that used in the formula are discussed. In Section 3, a method used to detect the grid corners and two local tangents is proposed based upon Harris corner detector [16]. The procedure and experimental result are presented. In Section 4, experimental results are shown and the errors in surface orientation are discussed. In Section 5, conclusion and future work are presented.

2. SURFACE ORIENTATION FROM TWO EDGE DIRECTIONS

Consider image point $A''(x, y)$ on the image plane, which is induced by the projection ray from one intersection point *A* on the pattern via surface point *A'* on the inspected surface, as illustrated by Figure 2. The illumination direction plus the checker board edge direction defines a plane referred to as *SPP*(*x, y*) (the *Shifting Projection Plane* associated with image position (*x, y*)). Suppose the surface normal of the inspected surface at point *A'* is $\mathbf{n}(x, y)$. $\mathbf{n}(x, y)$ comes with a tangent plane of the surface at *A'*. Note that amidst all the many tangents of the inspected surface on such a tangent plane, a particular one $\bar{\mathbf{t}}$ is contained by *SPP*(*x, y*). It is this tangent $\bar{\mathbf{t}}$ that determines the direction of the image flow at position (x, y) on the image. In fact $\bar{\mathbf{t}}$ together with the optical center O_2 of the camera defines a plane, which we refer to as *IFP(x, y)* (the *Image Flow Plane* associated with image position (x, y)). It is the intersection of *IFP(x, y)* and the image plane that defines exactly the direction by which the image flow moves at position (x, y) on the image. Define f_1 to be the image flow direction. Obviously, it can be obtained from the distorted continuous edge it locates. Define n_{11} to be the surface normal of *SPP*; n_{12} to be the surface normal of *IFP*. So the tangent t_1 can be obtained by the cross product of n_{11} and n_{12}:

$$\vec{t_1} = \overrightarrow{n_{11}} \times \overrightarrow{n_{12}} \tag{1}$$

Similarly, we can get the other direction edge:

$$\vec{t_2} = \overrightarrow{n_{21}} \times \overrightarrow{n_{22}} \tag{2}$$

Finally, the surface normal of object point A' can be calculated by:

$$\vec{n} = \vec{t_1} \times \vec{t_2} \tag{3}$$

In Figure 2, two coordinate systems are defined, world coordinate system: $x_w y_w z_w$ and image coordinate system: $x_I y_I z_I$. The two coordinate systems can be related by a transfer matrix *T* after simple calibration.

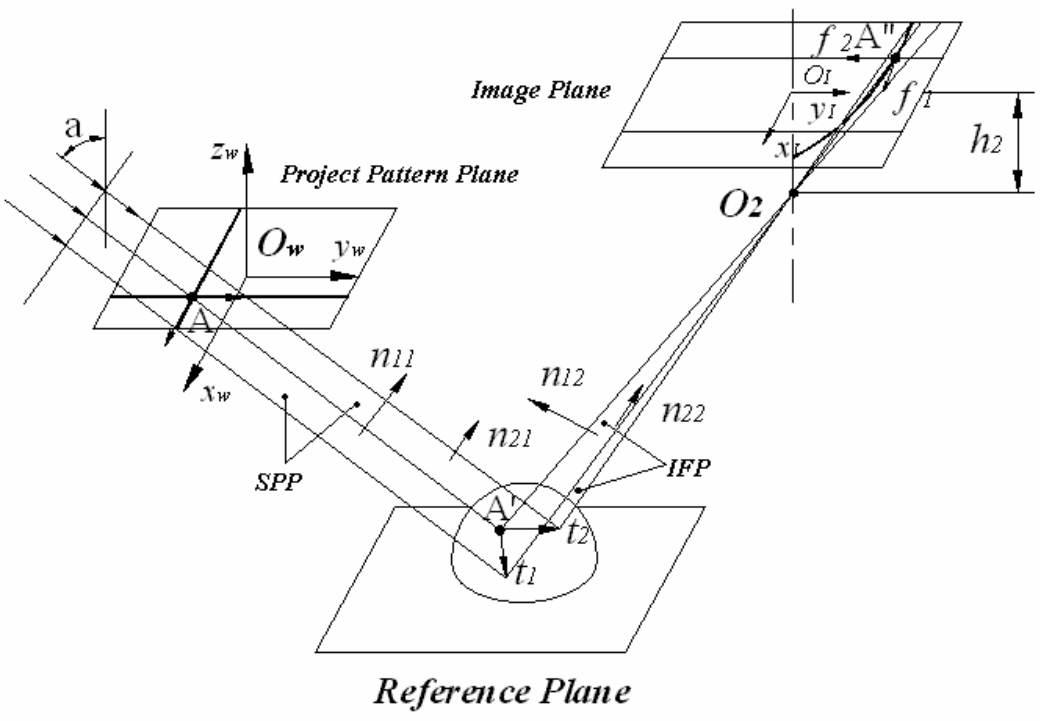

Figure 2. A checker board pattern is projected onto an object's surface. And the surface normal at grid corner can be derived from the two surface tangents.

In the pattern, if the block edges are parallel to *x* and *y* axis in image plane respectively, then the edges parallel to x_w will have maximum distortion. On the contrary, minimized edge distortion can be obtained in y_w direction. This will induce the method to a case of crabs. From Figure 2, it is easily to know *SPPy* and *IFPx* are almost overlap under this case, which lead to t_2 is not available. The pattern has to be rotated with an angle to resume the distorted strip edges in *y* direction. Normally, the rotation angle θ is 45°. The incident angle referred to α in the formula can be estimated from the positions of light source and reference plane. In Formula 5, h_2 denotes the value of focal length of the camera lens and can be obtained through calibration.

θ_1 and θ_2 are the tangential angles of the two block edges at the intersection point. They can be induced by the first order derivative of the fitted edge points. Then, the surface normal can be derived from the following formulas:

$$\overrightarrow{n_{11}} = \{\cos\theta, \sin\theta, \sin\alpha\cos\alpha\}; \qquad \overrightarrow{n_{21}} = \{-\cos\theta, \sin\theta, \sin\alpha\cos\alpha\} \tag{4}$$

$$\overrightarrow{n_{12}} = \{-\tan\theta_1, 1, (y_I - x_I \tan\theta_1)/h_2\}; \qquad \overrightarrow{n_{22}} = \{-\tan\theta_2, 1, (y_I - x_I \tan\theta_2)/h_2\} \tag{5}$$

Substituting the four vectors into Formula (3), surface normal can be derived simply. θ, α, h_2 are constant when the system is calibrated ready. It means n_{11} and n_{21} are independent to the image information. In other words, the surface normal result is only decided by n_{12} and n_{22}. Fatherly, they are decided by θ_1 and θ_2. So, the extracting result of block edges and the calculation of their tilt angle will decide the final result of surface normal value.

3. GRID CORNER AND SURFAE TANGENT EXTRACTION

When the pattern is projected onto an object, the straight block edges will be modulated by its surface. According to our method, surface normal at each intersection point is obtained by two tangents of the block edges passing through this point. So the problem can be depicted by following two steps:

(1) Extraction of grid corners (i.e., the intersection points).
(2) Detection of two block edges passing through the grid corner and computing their tangents.

Harris corner detector which proposed by Harris and Stephens has various applications in computer vision field. The idea of the Harris interest point detector is to find spatial locations where has significant changes in both directions. According to its principle, it is effective to the 'L'-type corners. As for the grid corner in checker board, it can be considered as a combination of several 'L'-type corners. Except some false corners caused by image noise, usually, more than one corner will be picked out around the grid corner point with an average error about 2 pixels as shown in Figure 3.b by using Harris corner detector directly.

To get the accurate grid corner localization and the tangents, one simple method based Harris corner detector is proposed. The procedure can be depicted by following steps:

(1) Detect all the corner points by Harris corner detector.
(2) Set a rectangle window around each corner, and select the corner has maximum corner response value in the window and discards the others.
(3) Assume P is the selected corner and C is a circle centered at P.
(4) Consider the intensity of C, set a threshold to judge the intensity jumping times n. If $n = 4$, P is considered as a grid corner.
(5) Assume A, B, C, D are the four jumping points, the new grid corner can be relocated to P', the intersection point of two lines: l_{AB} and l_{CD}.
(6) Two surface tangents t_1, t_2 can be induced by the first order derivative of l_{AB} or l_{CD} after fitting process. Simplified, to the planar or smooth surface, they can be appointed with the tangents of l_{AB} and l_{CD} directly.

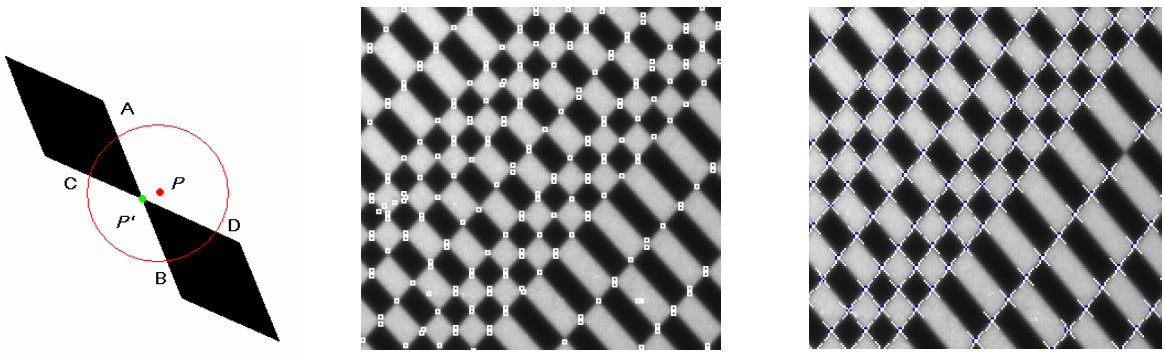

(a) (b) (c)

Figure 3. (a) A simple method to judge and get the accurate grid corner position. (b) The original Harris corner detection result. (c) Extracting result of grid corners and the two block edges with the improved method.

4. EXPERIMENTAL RESULTS

Surface normal is very local information and it is difficult to be measured directly. It means we can't get the ground truth in most case except some special objects, for example the ideal plane or ball and so on. According to the property of the target surface, our experiments can be divided into four types. First, we did a simple experiment on a planar surface. The potential error source is analyzed. Secondly, the pattern is projected onto a broach with several planar side faces. The result is analyzed and the statistic errors are presented. Subsequently, we did the experiment with a free form and unreflective object. Finally, we present the result on a specular solder paste surface.

Demission of most experimental objects we used is below 5mm. And each block size in the checker board pattern is about 0.1mm×0.1mm. The optical system is particular designed to acquire the best projection and image quality. The pattern is fastened to a fixture which is driven by a motor with the precision more than 1 micron. When the pattern shifts, the scene image of projection is grabbed synchronously. After calibration, the focal length of camera lens is about 40mm. The incident angle α is about 30° and the rotation angle θ is 45°.

4.1 Planar surface

Figure 4.a shows the image when the checker board pattern is projected onto a reference plane with surface normal vector [*0 0 1*] approximately. In the figure, the block edges are marked by two crossing white lines. The grid corners are the intersection points of the two edges. Some points maybe missed caused by image blurring and noise. Figure 4.b shows the 3D plot of the surface normal vectors (the arrows) at each grid corner (the circles). Statistic result shows the mean absolute angle error between exact vector [*0 0 1*] and the reconstructed normal vectors is 1.89°. The standard deviation value is about 2°.

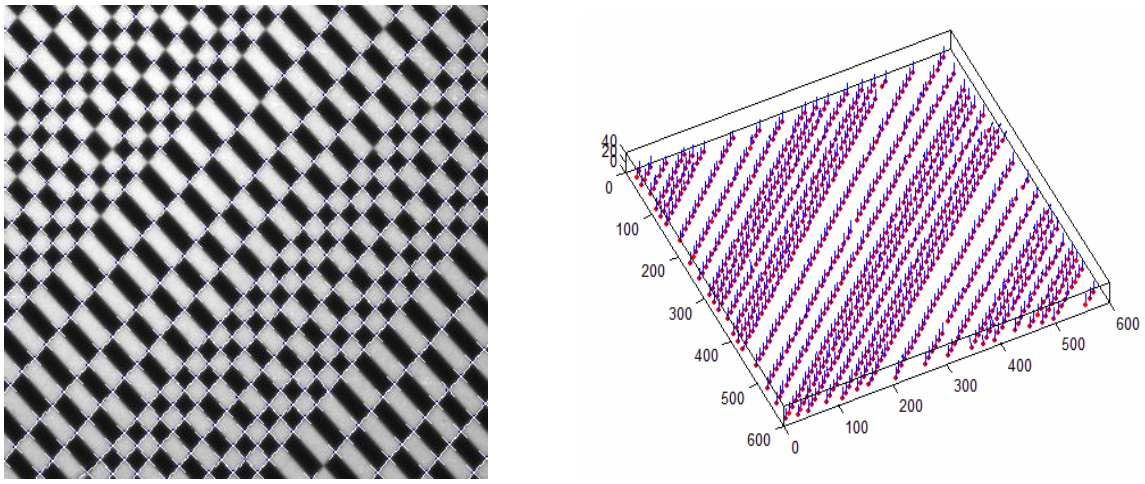

(a) (b)

Figure 4. (a) Extracting result of intersection points and block edges which marked with white cross lines in the projection image. (b) Needle map of surface normals.

4.2 Broach surface

In this experiment, we select a broach which has three planar side faces. When the pattern is projected, the whole scene can be separated into four planar regions. They are denoted by I, II, III, IV respectively as shown in Figure 5.d. The bottom of the broach is assumed planar. It is difficult to measure the surface normal of each side face directly. So, we set up an ideal 3D model for the broach. And the 'Ground Truth' of the surface normals are computed in the ideal model. All the intersection points are classified according to the region they belong to. The results are compared with the 'Ground Truth' as shown in Table 1.

Table 1. Statistic result of surface normal calculation.

Region	'Ground Truth'	Measured Result	Mad.	Std.
I	[0.67 -0.35 -0.65]	[-0.65 0.36 0.67]	2.4°	1.2°
II	[0.66 0.26 0.70]	[0.65 0.25 0.72]	3.4°	0.9°
III	[0.00 -0.86 0.52]	[0.02 -0.89 0.43]	5.3°	1.8°
IV	[0.0 0 .0 1.0]	[0.04 -0.03 0.99]	3.1°	0.3°

Mad.: mean absolute deviation; Std.: standard deviation;

From the result, we can see the mean absolute angle errors in most regions are below 5° except region-III. Since higher density will be obtained when the pattern is projected onto the sides with sharp tilt angle. A smaller circle should be selected to judge the jumping points. Shorten of searching radius has the quantizing error increase distinctly. The standard deviations of all regions are around 1°. The result shows the method is robust and accurate.

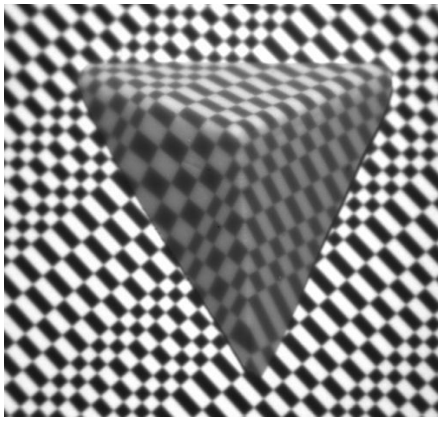

(a)

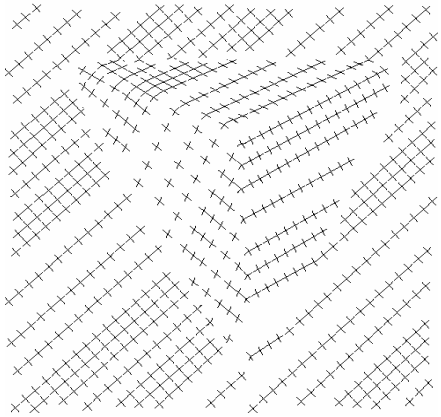

(b)

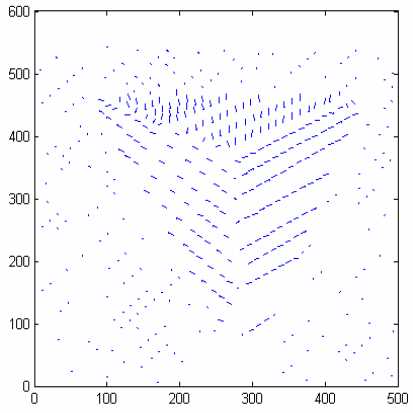

(c)

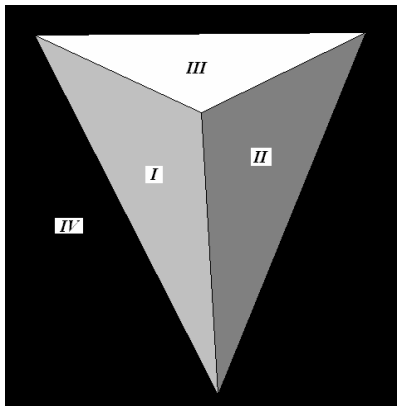

(d)

Figure 5. (a) Scene image when the pattern is projected onto a broach. (b) Extracting result of grid corners and block edges. (c) Needle map of surface normal in 3D space. (d) The ideal 3D model scene can be plot into four planar regions.

There are many sources of error when estimating the surface orientation, such as assumption of parallel projection, the accuracy of the strip edge location, lens calibration, camera pixel uniformity and so on. All these error sources can affect the position of strip edge points in image.

Normally, the sources of error can be generalized as following aspects:

(1) Illumination source: The effect of nonparallelism of the light planes for example the divergence angle is not considered. And it will make n_{11} different at different image positions.
(2) Surface property: Texture, reflection, and some sharp noise will cause errors in the result.
(3) Pattern orientation: Rotation angle θ is expected to be 45°, but error will exist during operation.
(4) Lens distortion: Image distortion appears especially in the image far from projection center.
(5) Quantizing error: Surface normal is calculated in terms of pixel units. It will cause some big errors especially the extracted strip edges are short.

4.3 Free-form surface

In this experiment, the checker board pattern is projected onto a free form object's surface as shown in Figure 6.a. The object's demission is around 5mm×4mm×1.5mm. The surface is unreflective and the projection result is satisfied except some blocks in the shadow region. The grid corners are marked with short cross lines as shown in Figure 6.b. The ground truth is not available as for this free-form object, so we can only judge it through observation and no quantitative statistic results are given in the paper. In general, most of the surface normal vectors point to the correct direction roughly as shown in Figure 6.c.

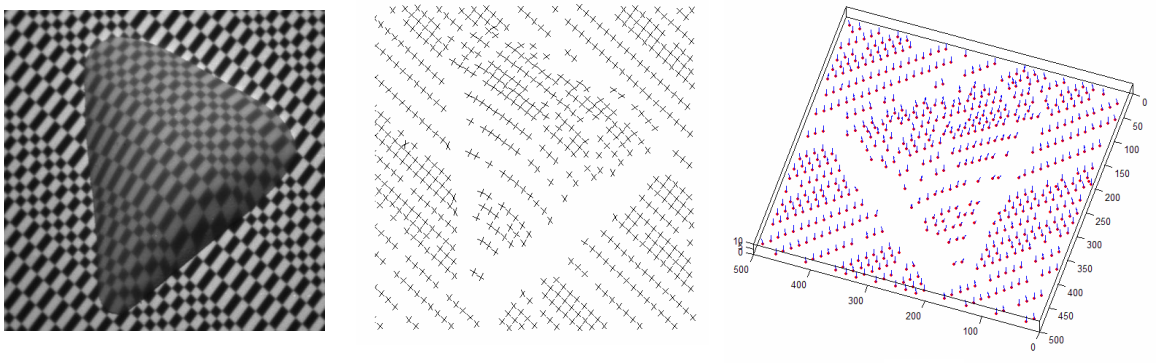

(a) (b) (c)

Figure 6. (a) Scene image when the pattern is projected onto a free-form object. (b) Extracting result of grid corners and block edges. (c) Needle map of surface normals.

4.4 Solder paste surface

From the above experimental results, we can see the method can obtain the grid corners and surface tangents effectively. And the experiment on planar surface demonstrates the surface normal calculation is accurate and robust. Anyway, these experiments are done under good surface conditions. As we know, reflection is always the obstacle in structured light system. It is very difficult to resume the strip edge information flooded by the saturation region. So it makes the orientation recovery more difficult. In order to get the images with good quality, we turn down the iris and utilize lower illumination strength. It can increase the depth of field and minimize the saturation region.

In order to test its performance under bad surface conditions especially the reflective surface. We project the pattern onto a solder paste of a circuit board as shown in Figure 7.a. From the image, we can see the contrast of block edge on the substrate is very blur. This caused by the absorption of light of the substrate material. The condition changes worse to the projection in shadow region. It is almost indistinguishable from the background. Saturation caused by high reflection especially at the solder peak destroyed the structure of the pattern. The texture on the substrate is mixed with the projection. All these negative factors as well as inhomogeneous background and strong noise on substrate aggravate the image quality and make the detection task difficult.

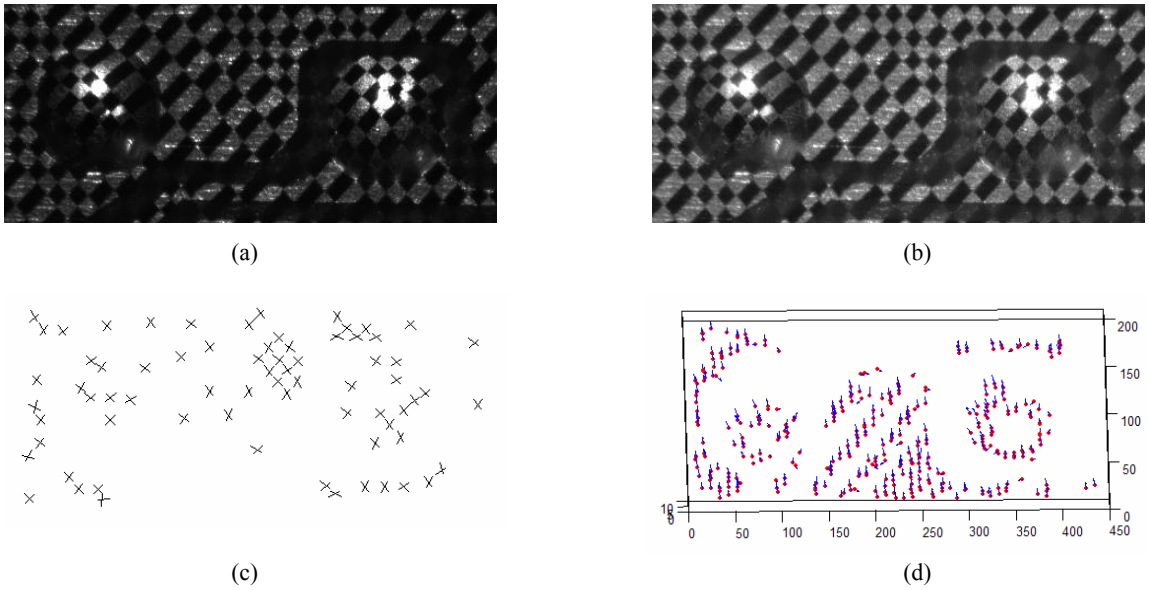

Figure 7. (a) Scene image when the pattern is projected onto a solder paste surface. (b) The image after preprocessing. (c) Extracting result of grid corners and block edges. (d) Needle map of surface normals.

In order to improve the image contrast and restrain the strong noise on substrate, preprocessing such as the histogram equalization and filtering are implemented before corner detection. The enhanced image as shown in Figure 7.b looks more sharp and clear than the original one. The size of experimental solder is about 2mm×2mm×0.75mm. Confined to the pattern size and optical system resolution, few blocks can be projected onto the solder surface. Consider the affection of saturation, substrate texture and noise, we have to increase the thresholds and make the retained corners as reliable as possible. Although some measures have been adopted in the algorithm, there still exist some false corners as shown in Figure 7.c. In order to get more dense data, the pattern is shifted 4 times and 5 images are grabbed synchronously. About 10% of the results have distinct deviation by observation.

5. CONCLUSION AND FUTURE WORK

Orientation recovery of specular micro-surface is a challenge work. It suffers the tiny size and reflective surface. In the structured light system, this phenomenon becomes more seriously. In the paper, we proposed a new method to calculate the surface normals through a binary checker board projection. The grid corner extraction and block edge detection methods are proposed as well. Real experiments are implemented to different surface types. The results show that the method is effective and robust. In the experiment of solder surface, most of the results are reasonable.

To get more accurate surface orientation, an optimized illumination source and optical system are expected to control the high reflection of solder surface. On the other hand, surface normal is a local value, and it is difficult to be measured directly. In most case, we can only judge it roughly. How to measure the result especially on the free-form object is also an important issue need to be concerned. Sub-pixel technique may be useful to increase the precision of surface tangents calculation. A look-up table associated with θ_1 and θ_2 is recommended to improve the speed of computation. Consideration of the error sources we mentioned can also improve the result.

ACKNOWLEDGMENTS

The work described in this paper was substantially supported by a grant from the Innovation and Technology Commission of Hong Kong Special Administrative Region, China, under an Innovation and Technology Fund with Project Code UIM/111.

REFERENCES

1. Sameh M. Yamany, Aly A. Farag, "An orientation independent free-form surface representation scheme for the purpose of objects registration and matching," IEEE Trans. on Pattern Analysis and Machine Intelligence, vol. 24, no. 8, August 2002.
2. S. Lavallee, R. Szeliski, "Recovering the position and orientation of free-form objects from image contours using 3D distance maps," IEEE Trans. Pattern Analysis and Machine Intelligence, vol. 17, pp. 378-390, April 1995.
3. C.S. Chua, R. Jarvis, "3D free-form surface registration and object recognition," International Journal of Computer Vision, vol. 17, pp. 77-99, 1996.
4. K. Ikeuchi, B. K. P. Horn. P. Sobalvarro, S. Nagata, "Determining grasp point using photometric stereo and the PRISM binocular stereo system," International Journal of Robotics Research, vol. 5, no. I, pp. 46-65, 1986.
5. B. K. P. Horn, M. J. Brooks, "Shape from Shading," MIT Press, Cambridge, 1989.
6. D. Blostein, N. Ahuja. "Shape from texture: Integrating texture-element extraction and surface estimation," PAMI, 11(12), pp. 1233–1251, 1989.
7. Peter Kovesi, "Shapelets correlated with surface normals produce surfaces," 10th IEEE International Conference on Computer Vision, vol. 2, pp. 994-1001, October 2005.
8. L.G. Brown, H. Shvayster, "Surface Orientation from projective foreshortening of isotropic texture autocorrelation," IEEE Trans. on Pattern Analysis and Machine Intelligence, vol.12, no.6, pp. 584-588, June 1990.
9. Neelima Shrikhande, George Stockman, "Surface orientation from a projected grid," IEEE Trans. on Pattern Analysis and Machine Intelligence, vol. II, no. 6, June 1989.
10. R. J. Woodham, "Photometric stereo: A reflectance map technique for determining surface orientation from image intensity," Proc. 22nd Int. Symp. SPIE, vol. 155, pp. 136-143, 1978.
11. K. Sugihara, K. Okazaki, F. Kaihua, N. Sugie, "Regular pattern projection for surface measurement," Proc. 2nd International Symp. Robotics Research, pp. 17-24, 1984.
12. S. Winkelbach, F. M. Wahl, "Shape from 2D edge gradients," Pattern Recognition, Lecture Notes in Computer Science 2191, pp. 377-384, 2001.
13. S. Winkelbach, F. M. Wahl, "Shape from single stripe pattern illumination," Pattern Recognition, Lecture Notes in Computer Science 2449, pp. 240-247, 2002.
14. M. Asada, H. Ichikawa, S. Tsuji, "Determining surface orientation by projecting a stripe pattern," IEEE Trans. on Pattern Analysis and Machine Intelligence, vol.10, no. 5, pp. 749-754, September 1988.
15. Arthur C. Sanderson, Lee E. Weiss, "Structured highlight inspection of specular surfaces," IEEE Trans. on Pattern Analysis and Machine Intelligence, vol.10, no.1, pp. 44-55, January 1988.
16. C. Harris, M. Stephens, "A combined corner and edge detector," Fourth Alvey Vision Conference, pp. 147-151, 1988.